Nuclear Inst. and Methods in Physics Research B 414 (2018) 84–98

Contents lists available at ScienceDirect

Nuclear Inst. and Methods in Physics Research B

journal homepage: www.elsevier.com/locate/nimb

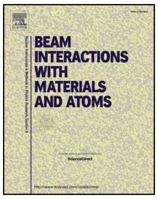

Chemical shift in $L\alpha$, $L\beta_1$, $L\beta_{3,4}$, $L\beta_{2,15}$, $L\gamma_1$ and $L\gamma_{2,3}$ emission lines of $_{47}$Ag, $_{48}$Cd and $_{50}$Sn compounds

Harpreet Singh Kainth[a,*], Ranjit Singh[a,b], Gurjot Singh[a], D. Mehta[a]

[a] Physics Department, Panjab University, Chandigarh 160014, India
[b] Department of Radiotherapy, PGIMER Chandigarh 160012, India

ARTICLE INFO

Keywords:
L emission lines
Chemical effect
Theoretical methods
Bond length
Relative line-width
CK process
Effective charge and WDXRF

ABSTRACT

Positive and negative shifts in *L* shell emission lines of $_{47}$Ag, $_{48}$Cd and $_{50}$Sn elements in different chemical compounds were determined from their recorded X-ray emission spectra in high resolution wavelength dispersive X-ray fluorescence (WDXRF) spectrometer. In $_{47}$Ag compounds, the measured energy shifts in $L\alpha$ X-ray emission line were in the ranges from (0.12 to 0.40) eV, $L\beta_1$ (0.27 to 0.36) eV, $L\beta_{3,4}$ (1.10 to 4.89) eV, $L\gamma_1$ (−0.09 to 1.13) eV and $L\gamma_{2,3}$ (−2.08 to 0.59) eV. Likewise, for $_{48}$Cd compounds, the estimated shifts in $L\alpha$ X-ray emission lines were in the range (−0.27 to 0.69) eV, $L\beta_1$ (0.50 to 2.06) eV, $L\beta_{2,15}$ (0.12 to 0.79), $L\beta_{3,4}$ (−0.62 to 1.79) eV, $L\gamma_1$ (0.10 to 1.35) eV and $L\gamma_{2,3}$ (−0.73 to 1.75) eV, while for $_{50}$Sn compounds, the measured shifts in $L\alpha$ X-ray emission lines were in the range of (0.02 to 1.81) eV, $L\beta_1$ (0.11 to 0.78) eV, $L\beta_{2,15}$ (0.15 to 1.40), $L\beta_{3,4}$ (0.17 to 2.01) eV, $L\gamma_1$ (0.09 to 1.08) eV and $L\gamma_{2,3}$ (0.17 to 1.40) eV respectively. The effective charges (q_P, q_S, q_L and q_B) were calculated by four different theoretical methods (Pauling method, Suchet method, Levine method and Batsonav method) and found to be linear dependent with the chemical shift. Further, the measured chemical shifts were correlated with bond length, relative line-width (FWHM), effective charge, electronegativity, number of ligands and Coster-Kronig (CK) transition processes.

1. Introduction

Chemical state analysis becomes more interesting topic for many researchers working in the spectroscopy field. The chemical effects can be studied by measuring either the shift in energies of characteristic X-ray photons [1–2], relative intensities of X-ray photons [3] or the formation of satellite lines [4]. X-ray photoelectron spectroscopy (XPS), energy dispersive X-ray fluorescence (EDXRF) spectrometers, photoemission spectroscopy (PES) and X-ray absorption near-edge structures (XANES) are the most common employed techniques used to identify the chemical state analysis in different compounds. All these techniques are non-destructive and bulk-sensitive to the chemical states of ir-radiating atoms, which provide useful insight of electron density, quantum states and atomic and electronic structures in the materials. During the formation of compound, metal atom transforms into a positive ion, results in change in the core binding energy of the electron. This deviation in the energy of a metal atom with respect to the different chemical compounds termed as chemical shift (ΔE), and is defined as $E_{metal} - E_{compound}$, where E_{metal} denotes central peak position of pure metal and $E_{compound}$ is the central peak position of the relevant compounds. However, having limited detector resolution and poor data reliability, these types of spectrometers suffer with lack of stability, electrostatic effects and uncertainty in the emission curves which requires large number of complex corrections [4,6–10].

To avoid these types of problems to some extent, wavelength dispersive X-ray (WDXRF) spectrometer with different ranging of high resolution crystals are used. Earlier many authors [5,11–15] reported the chemical effects in *K* and *L* shell emission lines of different low and medium Z elements. Chemical effect combination and their relative theoretical explanation on different chemical compounds, however, have not been established completely. Various factors like Coster-Kronig (CK) transitions, line-width (FWHM), effective charge and bond length etc are responsible for the cause of chemical shift. In past, Putila-Mantyla et al. [16] calculated the line-widths of $L\alpha_1$ and $L\beta_{1,3,4}$ emission lines in the atomic range $41 \leq Z \leq 50$ and showed sudden drop of L_1 line-width at $_{50}$Sn element due to the closing of L_1-$L_3M_{4,5}$ CK process. Likewise CK transitions, effective charge also plays an important role in chemical shift. Many researchers [17–22] studied the effective charge by various methods and techniques to show their impact on the chemical shift.

In the present work, our objective is to study the cause of chemical shift in *L* shell emission lines of different $_{47}$Ag, $_{48}$Cd and $_{50}$Sn

---

* Corresponding author.
E-mail address: harpreet.2january@gmail.com (H. Singh Kainth).

http://dx.doi.org/10.1016/j.nimb.2017.10.027
Received 14 August 2017; Received in revised form 23 October 2017; Accepted 24 October 2017

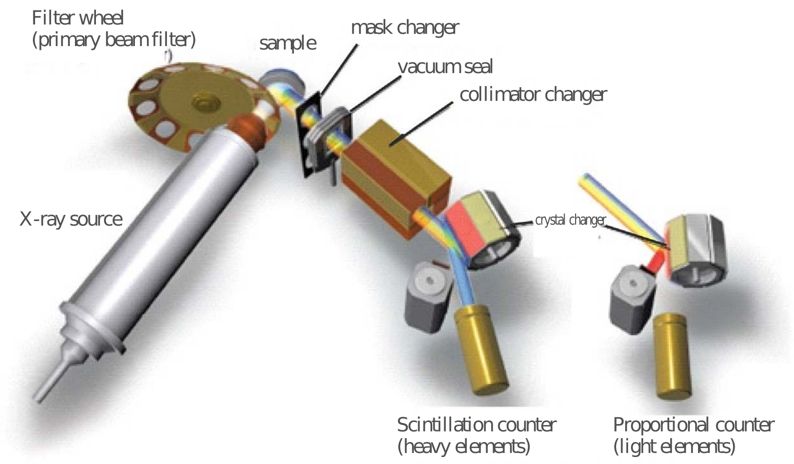

Fig. 1. The schematic diagram of S8 TIGER WDXRF X-ray tube setup (situated at Panjab University Chandigarh).

Table 1
Represents the oxidation state, manufacture's name and nearest bond distance of $_{47}$Ag, $_{48}$Cd and $_{50}$Sn compounds.

Compounds	Oxidation state	Manufacturer	Bond distance (Å)
Ag foil	0	Micromatter, Deer Harbor, WA	–
AgCl	+1	CDH Lab. Reagent	2.365
AgBr	+1	CDH Lab. Reagent	2.528
AgI	+1	CDH Lab. Reagent	2.737
Cd foil	0	Micromatter, Deer Harbor, WA	—
$CdCO_3$	+2	CDH Lab. Reagent	2.023
CdB_4O_7	+2	CDH Lab. Reagent	2.027
$Cd_3(PO_4)_2$	+2	CDH Lab. Reagent	2.125
$CdCl_2$	+2	CDH Lab. Reagent	2.404
CdI_2	+2	CDH Lab. Reagent	2.769
CdO	+2	CDH Lab. Reagent	1.813
CdS	+2	CDH Lab. Reagent	2.035
Sn foil	0	Micromatter, Deer Harbor, WA	–
SnF_4	+4	Sigma Aldrich	1.890
SnF_2	+2	Sigma Aldrich	1.943
SnO	+2	Sigma Aldrich	1.771
SnO_2	+4	Sigma Aldrich	1.981
$Sn(CrO_4)_2$	+4	Sigma Aldrich	2.765
$SnCl_2$	+2	Sigma Aldrich	2.355

compounds. The effective charges calculated by different methods and their role are also discussed.

2. Experimental details

2.1. Instrumentation

The chemical shifts in *L* shell of different chemical forms of $_{47}$Ag, $_{48}$Cd and $_{50}$Sn elements were measured on a high performance WDXRF spectrometer (Model: S8 TIGER, Bruker, Germany). The spectrometer was equipped with an Rh anode X-ray tube (4 kW, 60 kV and 170 mA), automatic collimator and beam changers operated under vacuum conditions. The schematic diagram of WDXRF apparatus was shown in Fig. 1. In WDXRF spectrometer, the high performance X-ray tube with narrow beam path and advanced analyzer crystals gave the highest intensity and fast data acquisition. The collimator masks were located between the sample and collimator to cut-off the radiation coming from the edge of the cup aperture. The space between the collimator plates restricted the maximum angle for divergence to the X-rays incident on the analyzing crystals. In the present measurement, LiF (2 0 0) high resolution analyzing crystal with 2d spacing (4.026 Å) is used. The Al filters of different thickness were used to avoid the contribution from bremsstrahlung radiations. The characteristic lines of different energies emitted from the sample were diffracted into different directions by the analyzing crystals. The diffracted characteristic lines were further detected by scintillation counter and proportional counter. For analysis procedure, SPECTRA ^{plus} software automatically corrected all matrix effects, measurement of calibration set, mathematical data processing and optimal calibration equations based on the fundamental parameters. During measurement, WDXRF spectrometer was evacuated down to ~15 Pa and temperature was stabilized at 37 °C. The typical acquisition time for each spectrum was 20 min. Each compound was analyzed at least five times to check the reproducibility. The abscissa axis of a chart was displayed in the 2θ angle with step size of 0.046° and step time of 0.15 s. In the present study, the abscissa axis was converted into the energy (eV) with the use of Bragg's law given by

$$n\lambda = 2d\sin\theta \tag{1}$$

where 'λ' is the wavelength of the X-ray, 'd' is the inter-atomic spacing between two layers of crystals, 'θ' is the angle between incident rays and surface normal to the crystal and 'n' is the order of diffraction pattern. The information about manufacturer, oxidation state and bond length of central metal atom in the compounds are given in Table 1. All the fine powder samples were spread uniformly on mylar film (~2 µm thickness). The given powder samples were then placed on the top of sample holder cup and thin mylar film was put on the top of the powder samples. Samples were analyzed in plastic cups using mylar film as base. The standard thin foils were measured as such as received from Micro-matter, Deer Harbor, WA, US.